Scattering Parameters for the Keefe Clarinet Tonehole Model

Gary P. Scavone & Julius O. Smith III

Center for Computer Research in Music and Acoustics (CCRMA), Department of Music, Stanford University, Stanford, California 94305 USA

Abstract

The clarinet tonehole model developed by Keefe [1981] is parametrized as the cascade of a series reactance, a shunt complex impedance, and another series reactance. The transmission matrix description of this two-port tonehole model is given by the product of the transmission matrices for each of the three impedances. For implementation in a digital waveguide model, these "lumped" parameters of the Keefe tonehole model must be converted to traveling-wave scattering parameters. Such formulations have recently appeared in the literature [Välimäki *et al.*, 1993] based on a three-port digital waveguide junction loaded by an inertance as described in Fletcher and Rossing [1991]. The scattering parameters of any high quality tonehole model are frequency dependent and therefore require a filter-design problem to be solved. This paper investigates a "four-filter" form for the Keefe tonehole scattering junction, as well as an improved one-multiply, one-filter three-port digital waveguide junction implementation.

1 THE TWO-PORT TONEHOLE MODEL

Keefe [1981, 1990] presents a model of a single woodwind tonehole unit in terms of a symmetric T section transmission matrix of series and shunt impedance parameters, as shown in Fig. 1. The series impedance

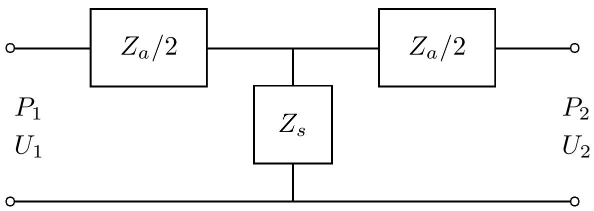

Figure 1: T section transmission-matrix representation of the tonehole.

terms, Z_a, result from an analysis of anti-symmetric pressure distribution, or a pressure node, at the tonehole junction. In this case, volume flow is symmetric and equal across the junction. The shunt impedance term, Z_s, results from an analysis of symmetric pressure distribution, or a pressure anti-node, at the tonehole, so that pressure is equal across the junction. The transmission matrix which results under this analysis is given by

$$\begin{bmatrix} P_1 \\ U_1 \end{bmatrix} = \begin{bmatrix} 1 & Z_a/2 \\ 0 & 1 \end{bmatrix} \begin{bmatrix} 1 & 0 \\ Z_s^{-1} & 1 \end{bmatrix} \begin{bmatrix} 1 & Z_a/2 \\ 0 & 1 \end{bmatrix} \begin{bmatrix} P_2 \\ U_2 \end{bmatrix} = \begin{bmatrix} 1 + \frac{Z_a}{2Z_s} & Z_a\left(1 + \frac{Z_a}{4Z_s}\right) \\ Z_s^{-1} & 1 + \frac{Z_a}{2Z_s} \end{bmatrix} \begin{bmatrix} P_2 \\ U_2 \end{bmatrix}. \quad (1)$$

Based on the approximation that $|Z_a/Z_s| \ll 1$, Eq. (1) can be reduced to the form

$$\begin{bmatrix} P_1 \\ U_1 \end{bmatrix} = \begin{bmatrix} 1 & Z_a \\ Z_s^{-1} & 1 \end{bmatrix} \begin{bmatrix} P_2 \\ U_2 \end{bmatrix}, \quad (2)$$

which is the basic tonehole unit cell given by Keefe for transmission-matrix calculations. The values of Z_a and Z_s vary according to whether the tonehole is open (o) or closed (c) as

$$\begin{aligned} Z_s^{(o)} &= Z_0(a/b)^2 \left(jkt_e + \xi_e\right), && \text{(3a)}\\ Z_s^{(c)} &= -jZ_0(a/b)^2 \cot(kt), && \text{(3b)}\\ Z_a^{(o)} &= -jZ_0(a/b)^2 kt_a^{(o)}, && \text{(3c)}\\ Z_a^{(c)} &= -jZ_0(a/b)^2 kt_a^{(c)}. && \text{(3d)} \end{aligned}$$

Definitions and descriptions of the various parameters in Eqs. (3a) – (3d) can be found in [Keefe, 1990]. The series impedance terms are characterized as negative inertances, which imply negative length corrections on both sides of the tonehole. If adjacent tonehole interactions are negligible, the single tonehole unit can be used to model an entire tonehole lattice as well. Internal tonehole interactions, which in general are much greater than external interactions, can be considered insignificant if the holes are separated by more than two times the main bore diameter [Keefe, 1983].

To render these relationships in terms of traveling-wave scattering parameters, it is necessary to transform the plane-wave physical variables of pressure and volume velocity to traveling-wave variables as

$$\begin{bmatrix} P_1 \\ U_1 \end{bmatrix} = \begin{bmatrix} P_1^+ + P_1^- \\ Z_0^{-1}\left(P_1^+ - P_1^-\right) \end{bmatrix}, \qquad \begin{bmatrix} P_2 \\ U_2 \end{bmatrix} = \begin{bmatrix} P_2^+ + P_2^- \\ Z_0^{-1}\left(P_2^+ - P_2^-\right) \end{bmatrix}, \tag{4}$$

where Z_0 is the characteristic impedance of the cylindrical bore, which is equal on both sides of the tonehole. Waveguide pressure variables on both sides of the tonehole are then related by

$$\begin{bmatrix} P_1^- \\ P_2^+ \end{bmatrix} = \begin{bmatrix} \mathcal{R}^- & \mathcal{T}^- \\ \mathcal{T}^+ & \mathcal{R}^+ \end{bmatrix} \begin{bmatrix} P_1^+ \\ P_2^- \end{bmatrix}, \tag{5}$$

where

$$\begin{aligned} \mathcal{R}^- = \mathcal{R}^+ &= \frac{4Z_aZ_s + Z_a^2 - 4Z_0^2}{(2Z_0 + Z_a)(2Z_0 + Z_a + 4Z_s)} \approx \frac{Z_aZ_s - Z_0^2}{Z_aZ_s + 2Z_0Z_s + Z_0^2}, && \text{(6a)}\\ \mathcal{T}^- = \mathcal{T}^+ &= \frac{8Z_0Z_s}{(2Z_0 + Z_a)(2Z_0 + Z_a + 4Z_s)} \approx \frac{2Z_0Z_s}{Z_aZ_s + 2Z_0Z_s + Z_0^2}, && \text{(6b)} \end{aligned}$$

calculated using Eqs. (1) and (4) and then making appropriate simplifications for $|Z_a/Z_s| \ll 1$. Figure 2 depicts the waveguide tonehole two-port scattering junction in terms of these reflectances and transmittances. This is a "four-filter" structure [Scavone and Smith, 1997]. A one-filter form is also possible [Smith and Scavone, 1997].

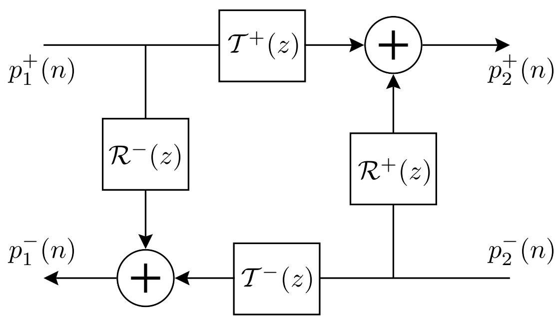

Figure 2: Digital waveguide tonehole two-port scattering junction in four-filter form.

The two-port waveguide tonehole scattering junction of Fig. 2 can be efficiently implemented using digital waveguide techniques [Smith, 1992]. For such an implementation, it is necessary to convert the continuous-time reflectances and transmittances to appropriate discrete-time filter representations. In this study, use is made of an equation-error minimization technique [Smith, 1983, p. 47] which matches both frequency response magnitude and phase. This technique is implemented in *MATLAB*® by the function *invfreqz*. Figure 3 plots the responses of second-order discrete-time filters designed to approximate the continuous-time magnitude and phase characteristics of the reflectance for closed and open toneholes. The closed-hole reflectance is essentially a highpass filter with a single "resonance" at the first closed-tonehole cavity resonance frequency. Thus, low-frequency wave components are only slightly affected by the presence of the closed hole. High-frequency components near this resonance, however, may be significantly reflected in the presence of the closed hole. The open-hole reflectance has a lowpass characteristic, with its single "anti-resonance" corresponding to the first open-tonehole branch resonance frequency. Low-frequency wave components are thus strongly reflected at an open tonehole. The open-hole discrete-time filter was designed using Kopec's method [Smith, 1983, p. 46], in conjunction with the equation-error method. That is, a one-pole model $\hat{H}_1(z)$ was first fit to the continuous-time response, $H(e^{j\Omega})$. Subsequently, the inverse error spectrum, $\hat{H}_1(e^{j\Omega})/H(e^{j\Omega})$ was modeled with a two-pole digital filter, $\hat{H}_2(z)$. The discrete-time approximation to $H(e^{j\Omega})$ was then given by $\hat{H}_1(z)/\hat{H}_2(z)$. The first step of this design process captures the peaks of the spectral envelope, while the second step models the "dips" in the spectrum. These particular calculations were performed for a tonehole of radius $b = 4.765$ mm, minimum tonehole height $t_w = 3.4$ mm, tonehole radius of curvature $r_c = 0.5$ mm, and air column radius $a = 9.45$ mm. The results of Keefe [1981] were experimentally calibrated for frequencies less than about 5 kHz, so that the continuous-time responses evident in the figures are purely theoretical above this limit. Therefore, the discrete-time filter design process was weighted to produce better matching at low frequencies.

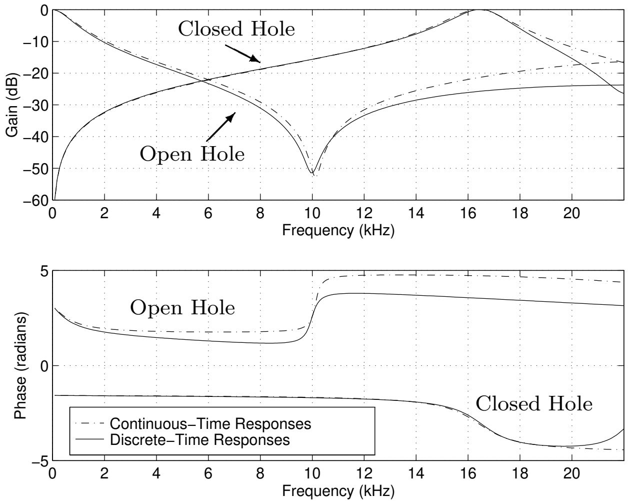

Figure 3: Two-port tonehole junction closed-hole and open-hole reflectances, derived from Keefe [1981] shunt and series impedance parameters. (top) Reflectance magnitude; (bottom) Reflectance phase.

Figure 4 plots the reflection function calculated for a six-hole flute bore, as described in [Keefe, 1990]. The upper plot was calculated using Keefe's frequency-domain transmission matrices, such that the reflection function was determined as the inverse Fourier transform of the corresponding reflection coefficient. This response is equivalent to that provided by Keefe [1990], though scale factor discrepancies exist due to differences in open-end reflection models and lowpass filter responses. The lower plot was calculated from a digital waveguide model using two-port tonehole scattering junctions. Differences between the continuous- and discrete-time results are most apparent in early, high-frequency, closed-hole reflections. The continuous-time reflection function was low-pass filtered to remove time-domain aliasing effects incurred by the inverse Fourier transform operation and to better correspond with the plots of [Keefe, 1990]. By trial and error, a lowpass filter with a cutoff frequency around 4 kHz was found to produce the best match to Keefe's results. The digital waveguide result was obtained at a sampling rate of 44.1 kHz and then lowpass filtered to a 10 kHz bandwidth, corresponding to that of [Keefe, 1990]. Further lowpass filtering is inherent from the first-order Lagrangian, delay-line length interpolation technique used in this model [Välimäki, 1995]. Because such filtering is applied at different locations along the "bore," a cumulative effect is difficult to accurately determine. The first tonehole reflection is affected by only two interpolation filters, while the

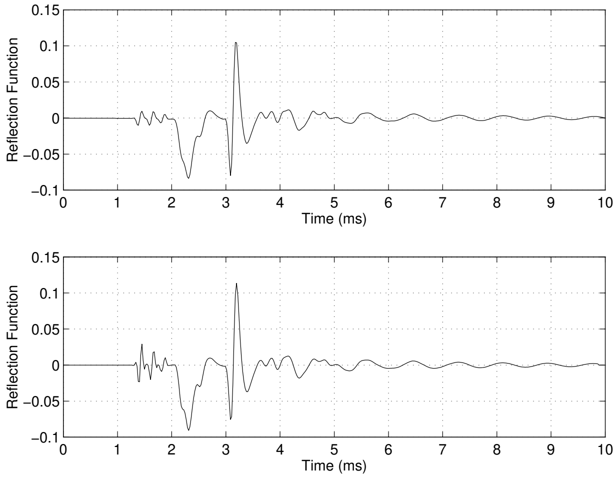

Figure 4: Reflection functions for note G (three finger holes closed, three finger holes open) on a simple flute (see [Keefe, 1990]). (top) Transmission-line calculation; (bottom) Digital waveguide two-port tonehole implementation.

second tonehole reflection is affected by four of these filtering operations. This effect is most responsible for the minor discrepancies apparent in the plots.

2 THE THREE-PORT TONEHOLE MODEL

A tonehole junction may also be represented in the digital waveguide context by a lossless three-port junction. The three-port junction models sound wave interaction at the intersection of the air column and tonehole, as determined by conservation of volume flow and continuity of pressure. Wave propagation within the tonehole itself can subsequently be modeled by another waveguide and the reflection/transmission characteristics at its end by an appropriate digital filter. This tonehole model is then attached to the appropriate branch of the three-port junction. The bore characteristic admittance Y_0 is equal on either side of the junction, while the real tonehole characteristic admittance is Y_{0th}. Because pressure is assumed constant across the three-port junction, this model neglects the series impedances of Fig. 1.

The three-port scattering junction equations for pressure traveling-wave components can be determined as

$$
\begin{aligned}
p_a^-(t) &= r_0 p_a^+(t) + [1+r_0]\, p_b^-(t) - 2r_0 p_{th}^-(t) && \text{(7a)}\\
p_b^+(t) &= [1+r_0]\, p_a^+(t) + r_0 p_b^-(t) - 2r_0 p_{th}^-(t) && \text{(7b)}\\
p_{th}^+(t) &= [1+r_0]\, p_a^+(t) + [1+r_0]\, p_b^-(t) - [1+2r_0]\, p_{th}^-(t), && \text{(7c)}
\end{aligned}
$$

where

$$
r_0 = \frac{-Y_{0th}}{Y_{0th} + 2Y_0} = \frac{-Z_0}{Z_0 + 2Z_{0th}}. \tag{8}
$$

A one-multiply form of the three-port scattering equations is given by

$$
\begin{aligned}
p_a^-(t) &= p_b^-(t) + w && \text{(9a)}\\
p_b^+(t) &= p_a^+(t) + w && \text{(9b)}\\
p_{th}^+(t) &= p_a^+(t) + p_b^-(t) - p_{th}^-(t) + w, && \text{(9c)}
\end{aligned}
$$

where

$$
w = r_0 \left[p_a^+(t) + p_b^-(t) - 2p_{th}^-(t) \right]. \tag{10}
$$

An implementation of these equations in shown in Fig. 5.

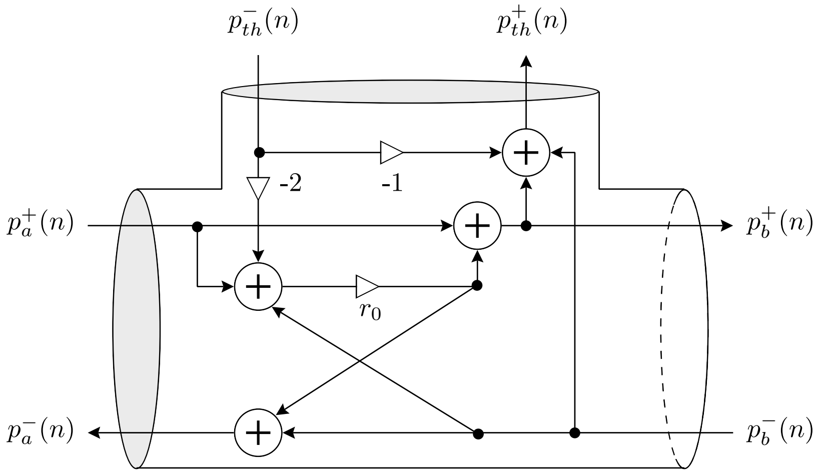

Figure 5: Tonehole three-port scattering junction implementation in one-multiply form.

To complete the digital waveguide three-port tonehole implementation, it is necessary to determine an appropriate model for the tonehole section itself, and then attach this model to the junction. It is possible to implement the tonehole structure as a short, fractional delay, digital waveguide and apply an appropriate reflectance at its end. Depending on the tonehole geometry, the reflectance at the end of an open tonehole may be determined from either a flanged or unflanged [Levine and Schwinger, 1948] pipe approximation. The far end of a closed tonehole is appropriately modeled by an infinite impedance (or a pressure reflection without inversion). Given typical tonehole heights, however, a lumped reflectance model of the tonehole, which accounts for both the propagation delay and end reflection is more appropriate and easily implemented with a single low-order digital filter. In this sense, incoming tonehole pressure $p_{th}^-(t)$ is calculated from the outgoing tonehole pressure $p_{th}^+(t)$ and the lumped tonehole driving point reflectance, while the corresponding pressure radiated from the open tonehole is given by convolution of $p_{th}^+(t)$ with the lumped tonehole section transmittance. Figure 6 plots the reflection function obtained for the six-hole flute bore implemented using digital waveguide three-port tonehole junctions. The lumped open-hole reflectance incorporates an unflanged characteristic, while the closed-hole reflectance which best matches the Keefe [1990] data includes no propagation delay within the side branch. Alternatively, the lumped tonehole reflectance filters can be designed from the shunt impedance parameters of Eqs. (3a) and (3b), thus taking advantage of the data of Keefe [1981]. The digital waveguide three-port tonehole junction implementation presented here corresponds to the two-port model when series impedance terms are neglected. In general, the series impedance terms are much less critical to the model performance than the shunt impedance, which is demonstrated by the similarity of the results for both implementations. Further, the series terms have more influence on closed-hole results than those for open holes [Keefe, 1981].

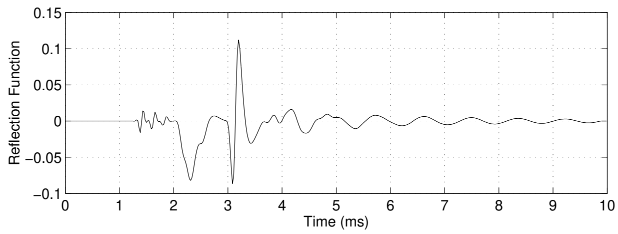

Figure 6: Reflection function for note G (three finger holes closed, three finger holes open) on a simple flute (see [Keefe, 1990]), determined using a digital waveguide three-port junction tonehole implementation.

3 CONCLUSIONS

Current theoretical models of woodwind finger holes can be accurately implemented in the digital waveguide domain. The two-port tonehole waveguide implementation requires four second-order filtering operations per tonehole (details regarding a one-filter form are to be published in the proceedings of the 1997 IEEE Workshop on Applications of Signal Processing to Audio and Acoustics, Mohonk Mountain House, New Paltz, NY). The three-port implementation requires one multiply and one filtering operation. The results for both implementations are very similar, despite the fact that the three-port model neglects the series impedance terms. A more complete and detailed analysis of this topic can be found in [Scavone, 1997].

References

Fletcher, N. H. and Rossing, T. D. (1991). *The Physics of Musical Instruments.* New York: Springer-Verlag.

Keefe, D. H. (1981). *Woodwind Tone-hole Acoustics and the Spectrum Transformation Function.* Ph.D. thesis, Case Western Reserve University.

Keefe, D. H. (1983). Acoustic streaming, dimensional analysis of nonlinearities, and tone hole mutual interactions in woodwinds. *J. Acoust. Soc. Am.*, 73(5):1804–1820.

Keefe, D. H. (1990). Woodwind air column models. *J. Acoust. Soc. Am.*, 88(1):35–51.

Levine, H. and Schwinger, J. (1948). On the radiation of sound from an unflanged circular pipe. *Phys. Rev.*, 73(4):383–406.

Scavone, G. P. (1997). *An Acoustic Analysis of Single-Reed Woodwind Instruments with an Emphasis on Design and Performance Issues and Digital Waveguide Modeling Techniques.* Ph.D. thesis, Music Dept., Stanford University. Available as CCRMA Technical Report No. STAN–M–100 or from ftp://ccrma-ftp.stanford.edu/pub/Publications/Theses/GaryScavoneThesis/.

Scavone, G. P. and Smith, J. O. (1997). Digital waveguide modeling of woodwind toneholes. In *Proc. 1997 Int. Computer Music Conf.*, Thessaloniki, Greece. Computer Music Association.

Smith, J. O. (1983). *Techniques for Digital Filter Design and System Identification with Application to the Violin.* Ph.D. thesis, Elec. Eng. Dept., Stanford University.

Smith, J. O. (1992). Physical modeling using digital waveguides. *Computer Music J.*, 16(4):74–91. Special issue: Physical Modeling of Musical Instruments, Part I.

Smith, J. O. and Scavone, G. P. (1997). The one-filter keefe clarinet tonehole. In *Proc. IEEE Workshop on Applied Signal Processing to Audio and Acoustics*, New York. IEEE Press.

Välimäki, V. (1995). *Discrete-Time Modeling of Acoustic Tubes Using Fractional Delay Filters.* Ph.D. thesis, Helsinki University of Technology, Faculty of Electrical Engineering, Laboratory of Acoustic and Audio Signal Processing, Espoo, Finland, Report no. 37.

Välimäki, V., Karjalainen, M., and Laakso, T. I. (1993). Modeling of woodwind bores with finger holes. In *Proc. 1993 Int. Computer Music Conf.*, pp. 32–39, Tokyo, Japan. Computer Music Association.